

Blood Flow in Idealized Vascular Access for Hemodialysis: A Review of Computational Studies

BOGDAN ENE-IORDACHE ¹ and ANDREA REMUZZI^{1,2}

¹Laboratory of Biomedical Technologies, Clinical Research Center for Rare Diseases Aldo e Cele Daccò, IRCCS – Istituto di Ricerche Farmacologiche “Mario Negri”, Via G.B. Camozzi 3, 24020 Ranica, BG, Italy; and ²Department of Management, Information and Production and Engineering, University of Bergamo, Dalmine, BG, Italy

(Received 13 December 2016; accepted 26 June 2017; published online 29 June 2017)

Associate Editors James E. Moore, Jr., Michael Walsh, and Ajit P. Yoganathan oversaw the review of this article.

Abstract—Although our understanding of the failure mechanism of vascular access for hemodialysis has increased substantially, this knowledge has not translated into successful therapies. Despite advances in technology, it is recognized that vascular access is difficult to maintain, due to complications such as intimal hyperplasia. Computational studies have been used to estimate hemodynamic changes induced by vascular access creation. Due to the heterogeneity of patient-specific geometries, and difficulties with obtaining reliable models of access vessels, idealized models were often employed. In this review we analyze the knowledge gained with the use of computational such simplified models. A review of the literature was conducted, considering studies employing a computational fluid dynamics approach to gain insights into the flow field phenotype that develops in *idealized* models of vascular access. Several important discoveries have originated from idealized model studies, including the detrimental role of disturbed flow and turbulent flow, and the beneficial role of spiral flow in intimal hyperplasia. The general flow phenotype was consistent among studies, but findings were not treated homogeneously since they paralleled achievements in cardiovascular biomechanics which spanned over the last two decades. Computational studies in idealized models are important for studying local blood flow features and evaluating new concepts that may improve the patency of vascular access for hemodialysis. For future studies we strongly recommend numerical modelling targeted at accurately characterizing turbulent flows and multidirectional wall shear disturbances.

Keywords—Vascular access, Arteriovenous fistula, Arteriovenous graft, Neointimal hyperplasia, Computational fluid dynamics (CFD), Wall shear stress (WSS).

Address correspondence to Bogdan Ene-Iordache, Laboratory of Biomedical Technologies, Clinical Research Center for Rare Diseases Aldo e Cele Daccò, IRCCS – Istituto di Ricerche Farmacologiche “Mario Negri”, Via G.B. Camozzi 3, 24020 Ranica, BG, Italy. Electronic mail: bogdan.ene-iordache@marionegri.it

INTRODUCTION

Description of the Condition

Chronic hemodialysis (HD) patients are a fragile population, already devastated by underlying uremia and/or diabetes and at high risk of cardiovascular events. If it is in good condition, their vascular access (VA), delivered by either native arteriovenous fistulae (AVF) or prosthetic arteriovenous grafts (AVG), guarantees the efficiency of HD treatment, making it a real lifeline for these patients. Fifty years after the first native AVF creation⁸ VA still remains a pervasive problem for HD patients and an unmet need for HD operators, which should be researched further and understood to prevent early and long-term failure of the shunt. Even though clinical guidelines^{57,72,79} recommend well-defined criteria to create the VA, a high early failure rate^{3,4} is found worldwide due to insufficient flow enhancement induced by stenotic lesions downstream from the anastomosis.

Geometry of the Vessels and Blood Flow in the VA

Native AVF can be constructed with different surgical techniques⁴⁰ to create the anastomosis between the vein and artery: (a) side artery to end vein (*side-to-end*), (b) end artery to end vein (*end-to-end*) and (c) side artery to side vein (*side-to-side*), as shown in Fig. 1. The AVG are created by connecting an artery with a vein *via* a prosthetic graft, which may be positioned under the skin in a closed-loop (Fig. 1d) or straight configuration. Naming rules for the fistula take into account the blood vessels involved and their location, e.g., lower arm radial–cephalic, upper arm brachial–cephalic AVF, *etc.* By convention, the exact

description of the anastomosis type (e.g., *side-to-end* or *end-to-side*) takes the direction of blood flow into account.³⁹ For example, in an AVF there is a *side-to-end* arterial anastomosis (Fig. 1e) and an *end-to-side* venous anastomosis (Fig. 1f). The nonuniform geometry near the anastomosis forces blood to change direction rapidly. In *side-to-end* anastomoses, blood flow is directed from the proximal artery (PA) to the vein, while the flow in the distal artery (DA) may be *retrograde* if blood is directed from the hand to the anastomosis, or *antegrade* if blood flows towards the hand.^{68,70} If the anastomosis is *end-to-end*, blood flows from the artery to the vein in a bending vascular structure. *Side-to-side* fistulae have natural flow directed towards the anastomosis in the distal vein (DV) due to venous valves (Fig. 1c), although it is possible to invert it by disrupting the initial venous valve using a vessel probe.³⁴ In such geometries, which are by nature vessels with sharp bends and large variations in a cross-sectional area, fast accel-

eration or deceleration of blood entails recirculation vortices and secondary flows, with energy dissipation and nonuniform hemodynamic shear stresses across the circumference of the vessel.

Neo-intimal Hyperplasia in the VA

Unfortunately, the VA may be harmed by several complications, such as thrombosis, stenosis, hand ischemia or high output cardiac failure.⁵⁰ Thrombosis is the major cause of failure of VA, the occlusion resulting from initial deterioration of the vessel wall due to neo-intimal hyperplasia (NH) lesions. In the pathogenesis of venous NH, there are initial or *upstream* events, which produce injury of the endothelial cell (EC) layer like surgical trauma, hemodynamic shear stress, or vessel wall damage due to needle punctures. *Downstream* events are the responses of the vascular wall at the endothelial injury that consist of a cascade of cellular mechanisms leading to leukocyte adhesion, migration of smooth muscle cells (SMC) from the media to the intimal layer and proliferation.⁶⁶ The reader should be aware that the meaning of the terms *upstream* and *downstream* in this setting regards the timeline of events in the pathogenesis of NH, and is in no way associated with their significance in fluid mechanics. Among the *upstream* events related to the pathogenesis of NH, this review deals only with hemodynamic factors believed to contribute to VA dysfunction. A brief overview of the most relevant developments regarding intimal hyperplasia in cardiovascular biomechanics research in general, and especially in the VA field, are introduced first.

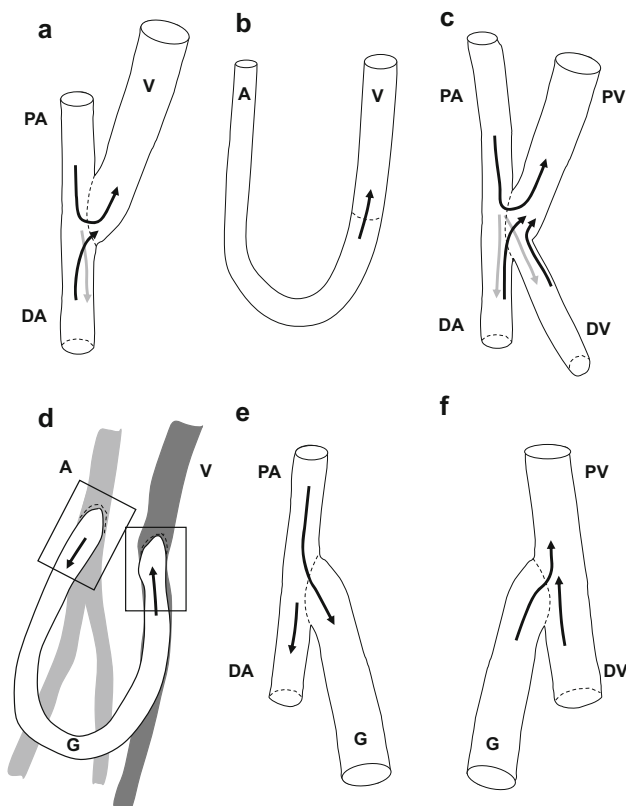


FIGURE 1. Drawings of the most used anastomotic geometries in VA. Top row, type of anastomoses in AVF: (a) *side-to-end*; (b) *end-to-end*; (c) *side-to-side*; bottom row, in AVG: (d) sketch of a closed-loop graft (G) that involves a; (e) *side-to-end* arterial anastomosis and a; (f) *end-to-side* venous anastomosis. Black arrows indicate the (more probable, while gray arrows the less probable) direction of blood flow. A, artery; DA, distal artery; DV, distal vein; G, graft; PA, proximal artery; PV, proximal vein; V, vein.

Relevant Achievements in the Field of Hemodynamics in the VA

Although the exact mechanisms of NH initiation and development remain unclear, turbulence-induced abnormal hemodynamic stresses are thought to trigger local wall thickening.^{7,48}

The Role of Multidirectional Disturbed Flow

A large amount of evidence has led to the hypothesis that the “disturbed flow” patterns in branch points and curvatures cause atherosclerotic lesions, whereas the laminar flow in the straight parts of the arterial tree is atheroprotective. Although frequently used, the term “disturbed flow” is vague enough and used in multiple settings with different connotations.²⁹ As currently used in the larger atherosclerosis community, *laminar disturbed flow* is defined as nonuniform and irregular, including recirculation eddies and changes in direction over time (*reciprocating flow*) and space (*flow separation*

and reattachment). The reciprocating flow in branch points and curvatures *in vivo* oscillates at the frequency of the cardiac cycle, modulating EC functions and vascular biology/pathobiology in vascular disease.¹⁴

Disturbed flow also results in postsurgical neointimal hyperplasia in the VA, where blood velocity is very high, giving rise to turbulent flow and audible bruits. On the venous wall, the turbulent flow induces highly oscillating, multidirectional shear stress, because the WSS vectors rotate very rapidly. This kind of *turbulent disturbed flow* regime has a very high frequency and differs essentially from the *reciprocating flow* that may develop in some focal points of the arterial side, which oscillates at the frequency of periodicity.²⁴ A direct relation between WSS and patterns of NH was demonstrated *in vivo* in pigs,^{41,63,64} in canines³⁵ and in mice⁸¹ animal models of AVF. In patients, the luminal shape at the site of stenosis is in the majority of cases off-center,⁶⁵ indicating a link with the WSS profile along the circumference of the vessel, which is nonuniform. Thus, as in other vascular pathologies,¹⁴ there are specific sites within the VA tree where stenoses develop, suggesting a link between local geometry, hemodynamics and NH formation. In native AVF for hemodialysis, the stenoses occur mostly on the venous segment, with the juxta-anastomotic vein (JAV) part as the most predominant site for radial-cephalic fistulae,^{6,62} the cephalic arch for the brachial-cephalic fistulae⁶² and the proximal vein segment for brachial-basilic fistulae.⁶² In AVG almost 80% of the stenoses occur at the venous anastomosis and only 4% at the arterial anastomosis.³⁷

Disturbed Flow Metrics and Computational Issues

In this setting, numerical modelling techniques such as computational fluid dynamics (CFD) are used to characterize the blood flow inside the VA and the patterns of wall shear stress (WSS) on its surface. In computational studies, zones affected by disturbed flow on the vascular wall may be localized by means of the so-called *hemodynamic wall parameters*. Some of these metrics are based on the magnitude of WSS, like the time-averaged wall shear stress (TAWSS), the oscillatory shear index (OSI) and the relative residence time (RRT), while others are based on the gradient of WSS, like the spatial gradient (WSSG), temporal gradient (WSSTG) or angle gradient (WSSAG).⁴⁴ The recent findings that oscillatory flow has pro-inflammatory effects when acting perpendicularly to the cell axis defined by their shape and cytoskeleton *in vitro*,^{61,80} as well as *in vivo* in the rabbit aorta,^{53,60} suggest that local multidirectional WSS vectors act as an *upstream event* for NH. In this context, the transversal WSS (transWSS) index proposed by Peiffer *et al.*⁶⁰ proved to be a valid

metric for characterizing the multidirectional flow, also in patient-specific AVF.^{7,20,24}

Regarding numerical grid resolution requirements, in CFD-related studies that aim to predict the outcome of a physical event for which experimental data are not available, the Fluids Engineering Division of ASME provided guidelines for calculating and reporting discretization error estimates through the Grid Convergence Index (GCI) method, based on the Richardson extrapolation.¹³ This should be the recommended procedure for estimating discretization errors also for computational studies in the VA.

Another challenging aspect in VA research is the existence the turbulence flow. Generally, turbulence may be completely simulated or modeled. Direct numerical simulation (DNS) is a computational technique that resolves all the details and scales of turbulence, i.e., the spatial and temporal evolution of the entire range of eddies, but is an extremely expensive approach, often requiring 10^8 – 10^{10} computational nodes and times extending to millions of CPU hours.⁴⁷ There have been studies using DNS, revealing transition to turbulence in the VA.^{46,48} A less expensive solution is to model the effects of small eddies and only resolve the large, most energetic eddies, through an approach called large eddy simulation (LES).⁹ More recent studies on cerebral aneurysms^{38,74} have shown that well-resolved spatially and temporally CFD simulations called “high-resolution” (HR-CFD) may detect the flow instabilities, otherwise not resolved by the common “normal-resolution” (NR-CFD). The HR-CFD approach is much less computationally expensive than DNS and probably equivalent to LES modelling, and has been used successfully in computational studies of VA.^{7,11,12,20,24,33}

Aim of the Review

In this special issue on VA, we have reviewed the existing literature by evaluating the computational studies of blood flow in three-dimensional models of VA for hemodialysis. This article is not intended as a comprehensive review of the numerous VA hemodynamics-related issues, but deals with computational studies realized in *idealized* models of either AVF or AVG anastomoses in the attempts to enlighten the flow phenomena that may be related to the failure of VA.

MATERIALS AND METHODS

We reviewed the published studies using numerical approaches to gain insights into the general flow field phenotype that develops in *idealized* models of the VA.

Literature Search Strategy

To retrieve the most representative computational studies performed in the VA setting, particularly in AVF or AVG, we conducted a nonsystematic search of PubMed with the keywords “Hemodialysis“, “Arteriovenous Fistula (modelling OR analysis)”, “Arteriovenous graft (modelling OR analysis)”, “Numerical Analysis, Computer-Assisted”[Mesh]”, and then we manually selected relevant articles, up until December 2016. The titles and abstracts of all potentially suitable studies were inspected and articles meeting the inclusion criteria were retrieved and reviewed.

Criteria for Considering Studies for This Review

Included in the review were computational studies that analyzed blood flow in idealized VA geometries. We did not include computational studies on patient-specific VA or studies that do not have a computational part. Although very similar in structure, we decided not to include in the review studies about vein grafts, which are exposed to a different hemodynamic regime when compared to the VA.⁴⁹ In addition, we did not include studies on central venous catheters (CVC) that are used in acute hemodialysis.

The studies selected for the review are presented in chronological order in Table 1. Included in the various outcomes investigated, are hemodynamic shear stress at the anastomosis, the helicity of the bulk flow, and the pressure drop over the anastomosis, or the hemodynamic effects of hemodialysis needles.

OVERVIEW OF THE COMPUTATIONAL STUDIES IN IDEALIZED VA

Arteriovenous Fistulae

Side-to-End AVF

In a parametric CFD study, Van Canneyt *et al.* investigated the impact of anastomosis size and angle on pressure drop and flow distribution⁷⁶ in a *side-to-end* AVF idealized model. Study parameters were the anastomosis cross-sectional area and the anastomotic angle. Starting with two reference cases with fixed flow split, pressure drop over the anastomosis was calculated for an arterial inflow in a range between 600 and 1200 mL/min. The pressure drop decreased with a larger anastomosis cross-sectional area and an angle wider than 43°, while it was almost constant for smaller angles. Subsequently, the same reference cases with fixed pressure boundary conditions were used to assess the flow split over the PV and DA. Although PA inflow increased for larger anastomosis areas, the overall flow split shifted almost totally to the PV.

When the anastomosis angle exceeded 58°, the PA inflow was not sufficient to deliver enough flow, leading to DA flow reversal.

Ene-Iordache *et al.*²³ performed a numerical study with the aim of investigating the hemodynamic flow field and the patterns of WSS in forearm radial-cephalic AVF. By using CFD simulations within idealized 3-D models of *side-to-end* they have found that WSS patterns depend on the flow split ratio and blood direction in the DA, i.e., antegrade or retrograde. Zones of disturbed flow localized by means of OSI and RRT were found on the anastomotic floor and on the inner wall of the JAV (Figs. 2a, 2b and 2d, 2e). These zones were located in the same sites where luminal reduction was documented in previous *in vivo* studies.^{6,71} Following this line of research, the same group²¹ studied whether the anastomosis angle might influence the pattern of disturbed flow, using a parametric CFD study. Their idealized model of wrist *side-to-end* radial-cephalic AVF resembled intraoperative dimensional and flow conditions of a newly created AVF. They used four equivalent AVF meshes with anastomotic angles of 30°, 40°, 60° and 90° and then localized the disturbed flow by means of the RRT metric, on the anastomotic floor and on the inner side of the JAV of all four models. Quantification of these areas and inference analysis showed that, the smaller the angle, the smaller the area of disturbed flow in idealized *side-to-end* radial-cephalic AVF.

Browne *et al.*¹¹ compared *in vivo* measurements of pressure distribution in two brachio-cephalic *side-to-end* AVF of hemodialysis treated patients against a representative idealized numerical model. They measured the pressure intra-operatively at stations located every 1 cm up to 6 cm into the vein, and in the distal and proximal segments of the artery. There was a distinct pressure drop (approximately 90 mmHg) between the arterial and venous segment, and this coincided with the well-known palpable thrill due to perivascular vibration observed *in vivo*. Constant flow simulations for an inlet Reynolds number of 1000 were advanced in time for 3 s and the first second of data was removed to eliminate the start up transients. By resolving the flow field with a fine time step (5×10^{-4} s) the authors observed fluctuations in the numerical signal due to flow instabilities arising at the anastomosis and in the near-venous area. These include also the oscillations of the pressure drop signal, which ranged from 58 to 76 mmHg, with a mean of 66 mmHg, a relatively good agreement (range of error between 8 and 10%) between the *in vivo* and CFD prediction. This study provided a benchmark of the pressure distribution within *side-to-end* AVF demonstrating that HR-CFD solutions are capable of

TABLE 1. Reviewed articles in chronological order, with the VA configuration and outcomes studied.

First author	Year	Type of VA	Anastomosis model	Numerical method	Outcome	Reference
Krueger U	2002	AVG	End-to-side	NR-CFD (Fluent)	Local hemodynamics in normal and patched anastomosis	42
Loth F	2003	AVG	Venous end-to-side	DNS (SEM)	Level and distribution of velocity fluctuations within the venous anastomosis	48
Van Tricht I	2006	AVG	A side-to-end V end-to-side	NR-CFD (Fluent)	Local hemodynamics at the arterial (A) and venous (V) anastomosis	78
Lee SW	2007	AVG	Venous end-to-side	DNS (SEM)	Transitional blood flow under various conditions of flow split	46
Niemann AK	2010	Wrist RC AVF	Side-to-side	NR-CFD (Comsol)	Flow patterns and hemodynamic wall parameters (OSI)	56
Van Canneyt K	2010	Lower arm RC AVF	Side-to-end	NR-CFD (Fluent)	Influence of anastomosis size and angle on pressure drop and flow distribution.	76
Ngoepe MN	2011	AVG	End-to-side	NR-CFD & FE (Fluent & Abaqus)	Fluid and structural anastomotic mechanics of a straight upper arm AVG	55
Ene-Iordache B	2012	Lower arm RC AVF	Side-to-end End-to-end	NR-CFD (FIDAP)	Flow patterns and hemodynamic wall parameters (OSI, RRT)	23
Ene-Iordache B	2013	Lower arm RC AVF	Side-to-end	NR-CFD (FIDAP)	Hemodynamic wall parameter (RRT) in different angled AVF	21
Fulker D	2013	HD needles	–	NR-CFD (Ansys Fluent)	Adverse effects of venous needle on the hemodynamics of fistulae	25
Van Canneyt K	2013	AVG	–	NR-CFD (Fluent)	Impact of a helical AVG design on the occurrence of favorable hemodynamic conditions at the V anastomosis	75
Hull JE	2013	AVF	Side-to-side	NR-CFD (Star-CCM+)	Flow patterns, pressure drops and hemodynamic WSS	31
Hoganson DM	2014	AVF	–	NR-CFD (Fluent)	Pressure drop over the AVF stenosis over a range of idealized stenoses	30
Sarmast M	2014	AVG	A side-to-end V end-to-side	HR-CFD (Fluent)	Local hemodynamics in two HD arteriovenous grafts: 8-mm tapered to 6-mm and straight 6 mm	67
McNally A	2014	AVG	Venous end-to-side	NR-CFD (Fluent)	Design of a modular anastomotic valve device that can isolate the graft between dialysis periods	52
Broderick SP	2015	AVG	Venous end-to-side	HR-CFD (Ansys Fluent)	Vein diameter and flow split ratio contribution in flow instability	9
Browne LD	2015	Upper arm BC AVF	Side-to-end	HR-CFD (Star-CCM+)	Validation of the in silico predicted pressure drop across AVF	11
Browne LD	2015	Upper arm BC AVF	Side-to-end	HR-CFD (Star-CCM+)	Numerical analysis of bulk flow parameters in the AVF	12
Iori F	2015	Wrist RC	Side-to-end	HR-CFD (Star-CCM)	How arterial curvature alters the blood flow and oxygen transport	33
Fulker D	2016	HD needles	–	NR-CFD (Ansys Fluent)	The hemodynamic effects of HD needle rotation and orientation	27
Kabinejadian F	2016	AVG	Side-to-side End-to-side	NR-CFD (Ansys CFX)	Sequential design of the venous anastomosis	36
Fulker D	2016	HD needles	–	HR-CFD (Ansys Fluent)	Hemodynamic effects of arterial and venous needles during HD session	26

AVF, arteriovenous fistulae; AVG, arteriovenous grafts; BC, brachial-cephalic; RC, radial-cephalic; NR-CFD, high-resolution CFD; HR-CFD, normal resolution CFD; VA, vascular access.

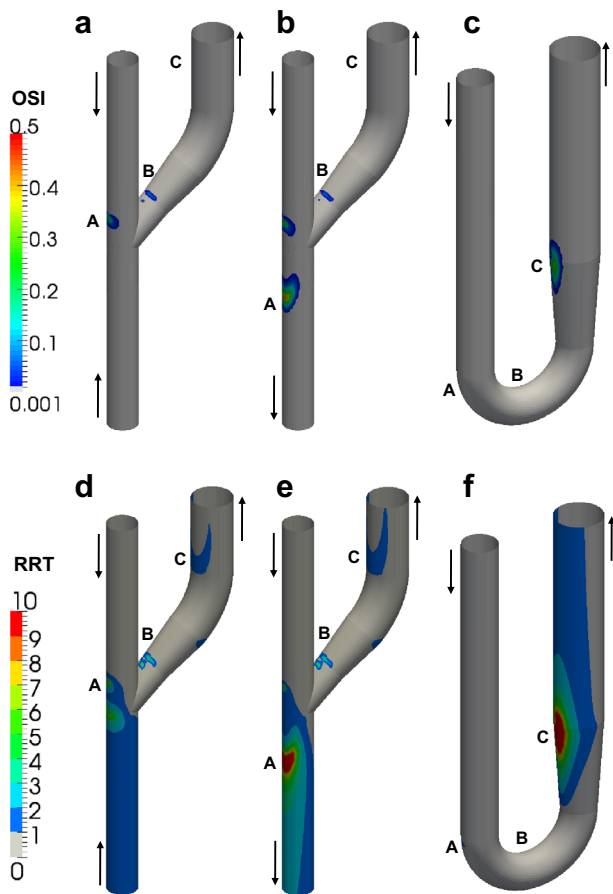


FIGURE 2. Plot of OSI and RRT on the AVF surface. Arrows indicate the direction of flow. (a and d) Side-to-end AVF with retrograde flow in the DA. (b and e) Side-to-end AVF with antegrade flow in the DA. (c and f) End-to-end AVF. Figure reprinted by permission from Oxford University Press.²³

replicating the abnormal physiological flow conditions induced by fistula creation.

Following the same research line, Browne *et al.*¹² investigated whether adequately resolved CFD might capture the flow instabilities within an idealized model of *side-to-end* AVF. In addition, an experimental model of the representative fistula was created and the pressure distribution within the model was analyzed experimentally and numerically using steady inlet conditions, and then a pulsatile simulation was run in order to assess the role of pulsatility on bulk flow. The flow within the venous segment exhibited transitional flow under both steady and pulsatile inlet conditions. High frequency velocity fluctuations developed in the AVF under pulsatile conditions, starting in the anastomosis and propagating in the JAV segment (Fig. 3). These fluctuations may impact EC function and contribute as an *upstream* event in the pathogenesis of NH, further contributing to the loss of VA functionality.

Iori *et al.*³³ investigated computationally, the effect of in-plane arterial curvature on blood flow and oxy-

gen transport in *side-to-end* idealized AVF configurations. The aim of the study was to understand how arterial curvature may affect blood flow and oxygen transport patterns, with a focus on how curvature alters the hemodynamic wall metrics known to correlate with NH. They used a constant (steady) flow at the inlet (equivalent Reynolds number of 800), advanced in time until transient start-up phenomena quit and only periodic physical fluctuations remained. For straight and inner AVF configurations the arterial flow was unsteady, despite the steady inflow, while for the outer configuration this was largely steady (Fig. 4). Venous flow was largely unstable for all configurations, except for the case of the smallest venous diameter (Fig. 4). Their findings imply that, if one subscribes to the hypothesis that disturbed flow causes NH, AVF should be formed *via* a vein graft onto the outer side of a curved artery in order to avoid NH. On the other hand, if one subscribes to the hypothesis that low WSS and/or wall hypoxia cause NH, AVF should be formed onto as straight as possible an artery or the inner side of a curved artery.

End-to-End AVF

The flow field in an idealized model of *end-to-end* AVF was investigated computationally by Ene-Iordache *et al.*²³ In this setting, the blood from the radial artery flows into the cephalic vein in a U-shape conduit and the curvature of the artery induces Dean flow in the bending tract. After the curvature, the flow impacts on the outer wall and a recirculation zone develops on the inner wall of the JAV. This type of flow phenotype results in low WSS regions on the inner wall of the cephalic vein, whereas high WSS develops on the inner and lateral walls of the bending artery at peak systolic flow. In addition, reciprocating disturbed flow, localized by means of OSI and RRT, developed on the inner wall of the vein after the anastomosis in idealized *end-to-end* AVF (Figs. 2c and 2f).

Side-to-Side AVF

Niemann *et al.*⁵⁶ performed a numerical study with the aim of investigating the hemodynamic flow field and the patterns of WSS in an idealized model of *side-to-side* wrist radial-cephalic AVF. They further validated the CFD results through comparisons with experimentally measured volume flows and velocity fields from ultrasound scans. Visual comparisons between ultrasound and CFD images showed good agreement. They found that disturbed flow localized through OSI developing at two distinct regions in the vein downstream from the anastomosis (Fig. 5).

Hull *et al.*³¹ also studied a wide range (matrix) of AVF anastomoses with CFD. Their goal was to

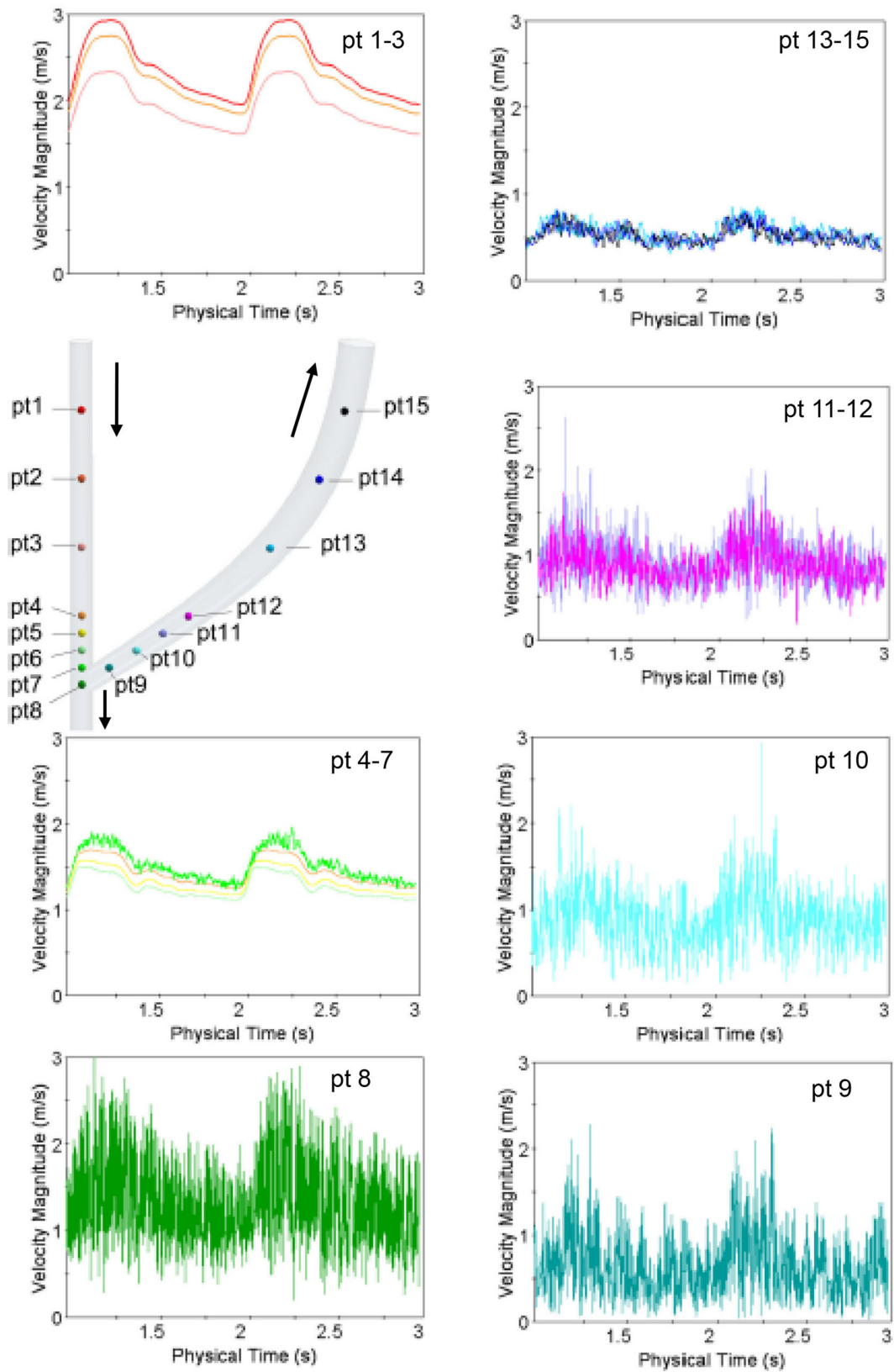


FIGURE 3. Velocity–time trace histories along centerline points (labeled 1–15) within the fistula model for a pulsatile flow solution with a mean flow rate of 1400 mL/min. Black arrows indicate the direction of blood flow. Reprinted by permission from Springer.¹²

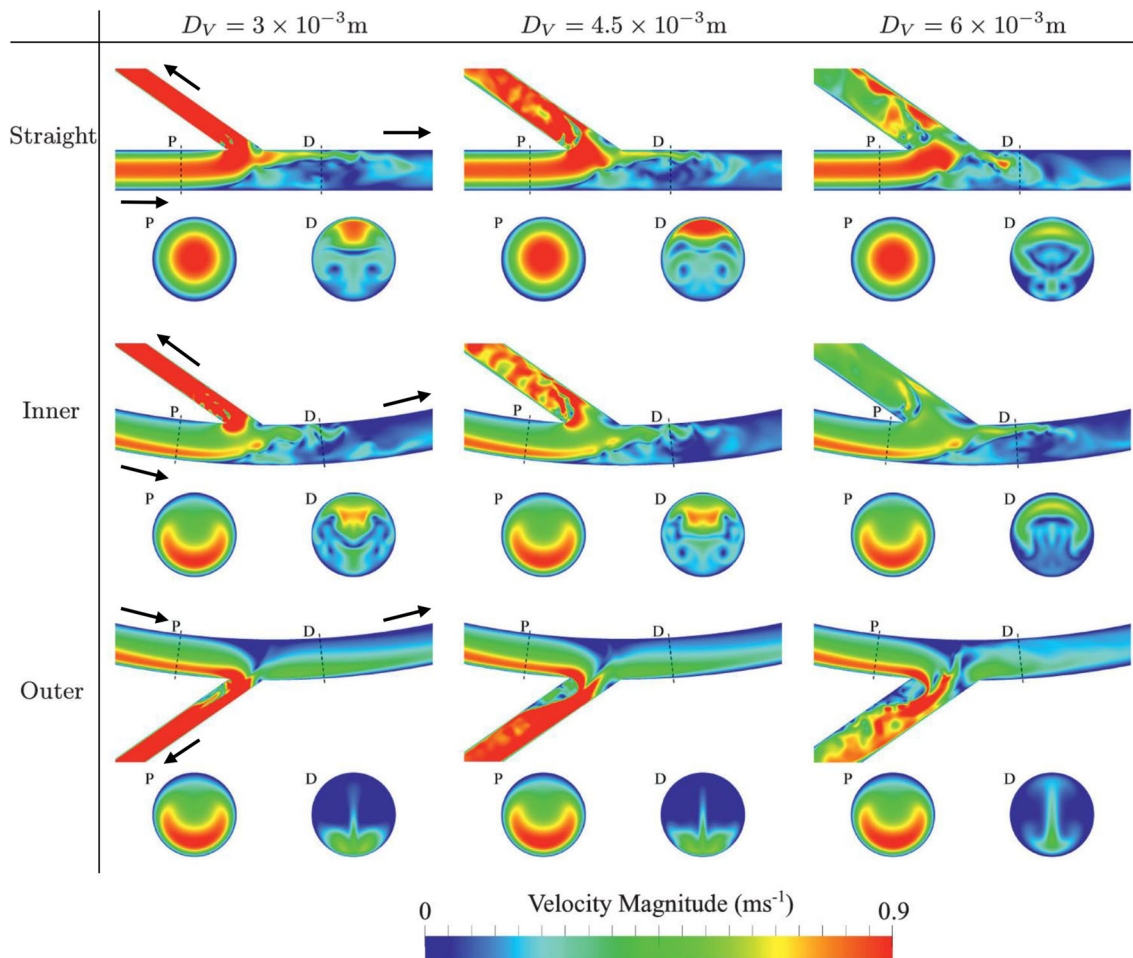


FIGURE 4. Temporal snapshots of velocity magnitude on the symmetry plane of idealized *side-to-end* AVF configurations, and on two planes orthogonal to the arterial centerline, positioned 1.2 cm proximal (P) and 0.6 cm distal (D) of the intersection between the arterial and venous centerlines. D_v , venous diameter; arrows indicate the direction of blood flow. Reprinted by permission from the authors.³³

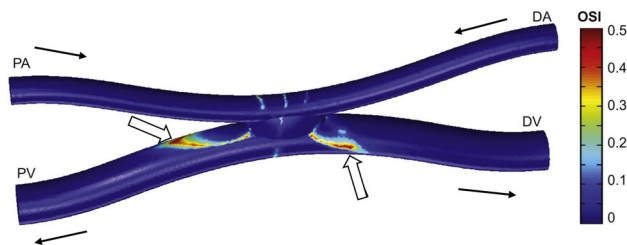


FIGURE 5. Plot of OSI in the vicinity of a *side-to-side* anastomosis. Maximum OSI values exceeded 0.4 at two distinct regions in the vein downstream to the anastomosis indicated by white arrows. Black arrows indicate the direction of blood flow. Reprinted by permission from Elsevier.⁵⁶

compare *side-to-side* with the more common *side-to-end* (45° and 90°) anastomosis configuration. They generated a matrix of 17 computer AVF models using different artery–vein diameter pairs. CFD simulations were performed at flow rates ranging from 600 to 1200 mL/min and mean arterial pressures from 50 to

140 mmHg. Their matrix CFD runs allowed them to obtain a wide range of pressure drops and venous outflows corresponding to any of these combinations. Moreover, the authors found that the most uniform WSS patterns occur in *side-to-side* anastomoses, followed by 45° and 90° *side-to-end* anastomoses (Fig. 6).

Pressure Drop over VA Stenoses

The hemodynamic significance of stenoses in VA was investigated by Hoganson *et al.*,³⁰ using a CFD to model the flow through AVF. Three-dimensional idealized models of clinically relevant stenoses, with the diameters ranging from 1.0 to 3.0 mm, and lengths between 5 and 60 mm within a generic AVF vein of 7 mm were generated. Eight patient-specific stenoses were also modeled and analyzed numerically, and the resulting blood flow calculations were validated through comparison with brachial artery flow measured by duplex ultrasound. The calculated flow rate

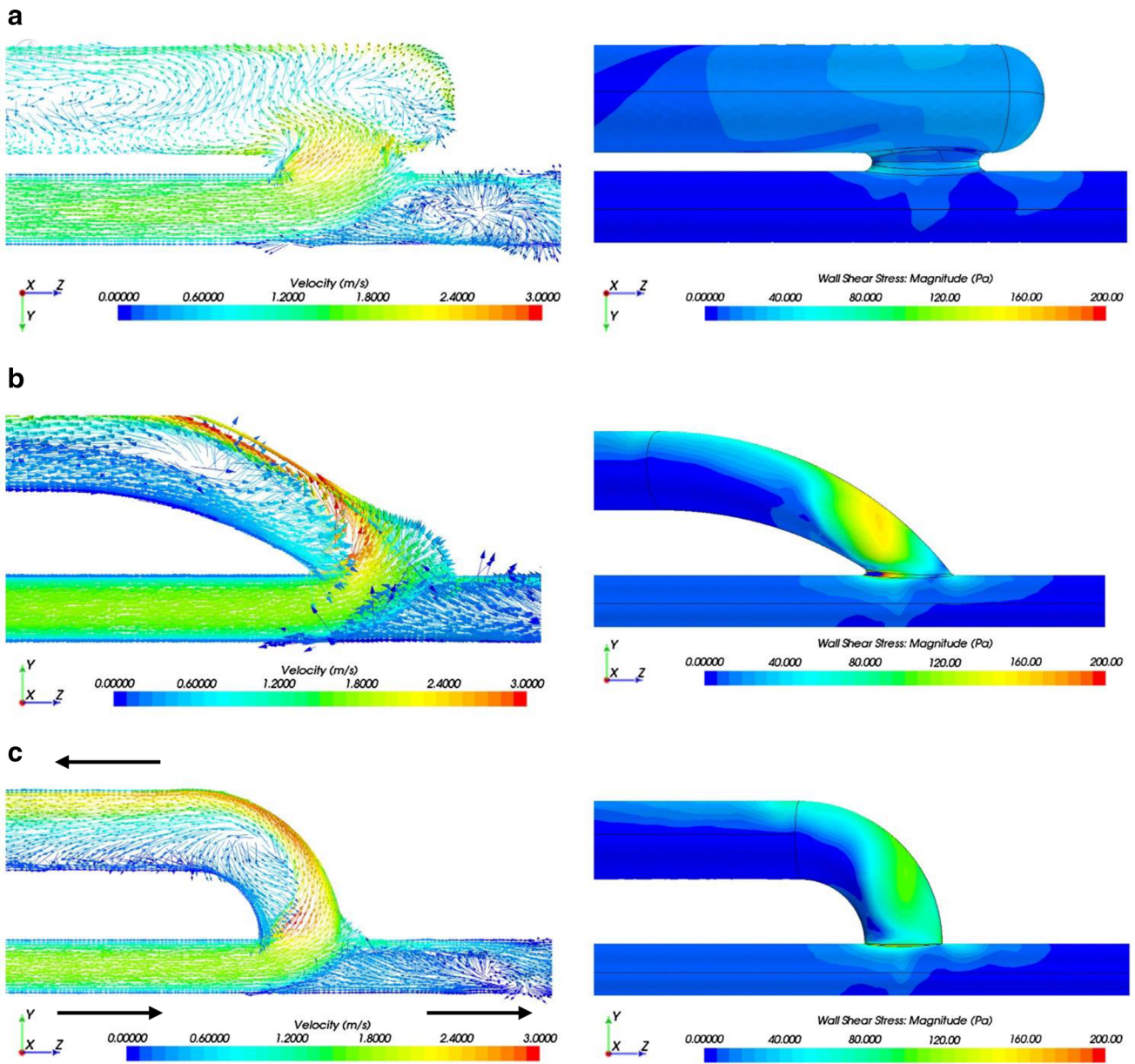


FIGURE 6. Paired velocity vector and surface plot of WSS at a constant flow rate of 900 mL/min for models of side-to-side (STS) (a) and 45° (b) and 90° (c) end-to-side (ETS). All anastomoses were ellipses of 6.0 × 4.0 mm in size. Note the uniform WSS in the STS configuration (a) compared with the marked variance in WSS in the 45° and 90° ETS configurations. Arrows indicate the direction of blood flow. Reprinted by permission from Elsevier.³¹

using CFD correlated with 20% of the ultrasound measured flow for five of eight patients, with a mean difference of 17.2% (range 1.3–30.1%). Their CFD study provided information on how to assess the functional significance of stenosis in VA dysfunction and to guide further intervention for VA salvation.

Arteriovenous Grafts

Krueger *et al.*⁴² investigated with NR-CFD a conventional and a patched form of venous *end-to-side*

anastomosis in idealized models. Their study aimed to investigate the effect of the design of venous anastomosis (see Fig. 1f) on hemodynamics. The main differences in geometry and size comprised not only the enlarged anastomotic room but also the curved design of the vein floor. Results of the numerical simulation showed a decrease of pressure on the floor of the host vein in the patch form (200 Pa) compared to conventional (372 Pa) anastomosis. They also found a reduction in peak systolic WSS from 5.9 Pa in the conventional form to 4.4 Pa in the patch form, on

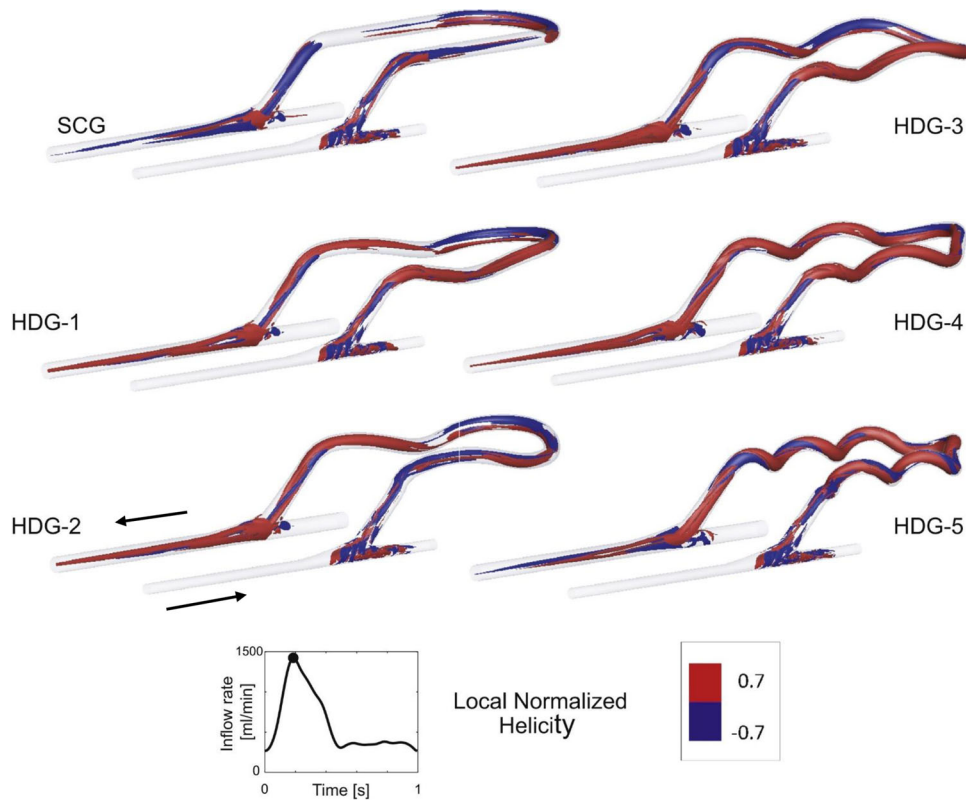


FIGURE 7. Isosurface of local normalized helicity (LNH) in the six helical graft designs, at peak systole. Positive and negative LNH values indicate counter-rotating helical structures induced by the grafts. The arrows indicate the direction of blood flow. Reprinted by permission from Elsevier.⁷⁵

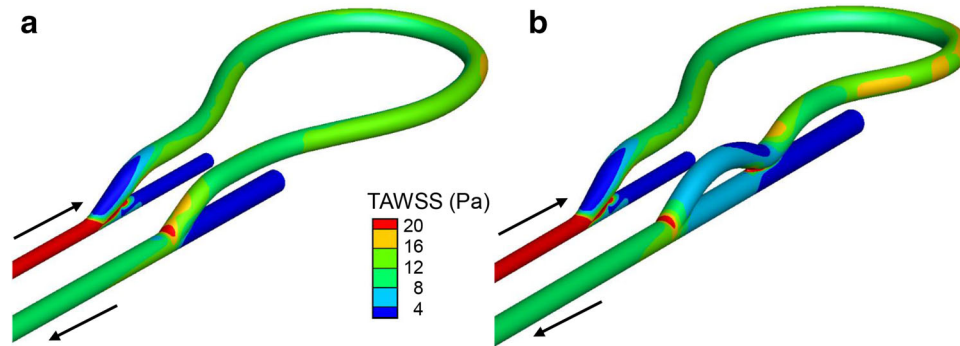


FIGURE 8. Distribution of TAWSS in the two VA models: (a) conventional end-to-side, (b) CSQA. The venous wall segment between the two (STS and ETS) anastomoses of the CSQA model provides a smooth transition of WSS along the venous wall between the low-WSS distal vein and the high-WSS proximal vein. Arrows indicate the direction of blood flow. Reprinted by permission from Taylor & Francis.³⁶

average an overall 50% reduction in WSS, and a more stable outflow within the patched form, compared to conventional anastomosis. Such favorable hemodynamic conditions may explain the decrease in NH formation in the patched anastomoses.

Loth *et al.*⁴⁸ investigated with DNS the steady flow at high Reynolds numbers ($Re = 1060$ and 1820) inside a venous anastomosis geometry. On the venous side the flow exhibited velocity field separation and weak turbulence that originated from the wall separation shear

layer. Their findings suggested a potential relationship between the associated turbulence-induced vein-wall vibration and the development of NH hyperplasia in AVG. On the same research line, Lee *et al.*⁴⁶ analyzed with DNS the transitional blood flow in an acute-angle venous anastomosis under various conditions of flow split ratio. Broderick *et al.*⁹ also studied, through HR-CFD, the transitional blood flow in a venous anastomosis with several conditions of flow split ratio and anastomosis angle. The results from both studies concur

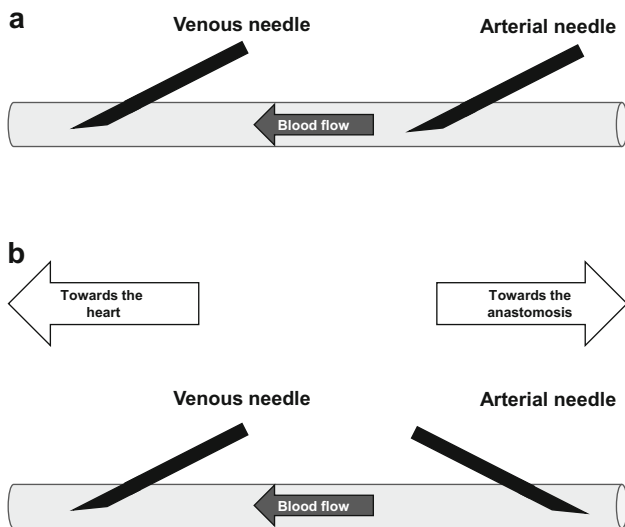


FIGURE 9. Positioning of cannulation needles on the venous part of the VA. The arterial needle may be inserted in either antegrade (a) or retrograde (b) direction. The venous needle should be inserted only in antegrade direction.

to suggest that vein diameter and/or flow split ratio contribute to turbulent generation, and thus Reynolds number cannot be used as a sole turbulent criterion in the arteriovenous anastomosis.

Ngoepe *et al.*⁵⁵ studied fluid and structural anastomotic mechanics of a straight PTFE upper arm graft. They used a combination of CFD and finite element (FE) models for arterial and venous anastomoses with different graft attachment angles. A mesh adaptation algorithm was developed to couple CFD and FE meshes and capture fluid structure interactions, enabling transfer of blood pressure predicted by CFD as loadings to the FE simulations. Their investigations of arterial and venous anastomotic *end-to-side* configuration indicated a slightly better performance of the 90° configuration over 135° arterial and 45° venous configurations.

Van Tricht *et al.*⁷⁸ investigated numerically whether different arterial anastomotic geometries result in different hemodynamics at the arterial and venous anastomosis of hemodialysis VA grafts. They studied two commercially available PTFE-grafts, a 6 mm cylindrical graft and a 4–7 mm tapered graft, both in a closed-loop configuration of the same length (340 mm), and assuming a mean volumetric flow rate of 1000 mL/min. The WSSG at the suture line of the arterial anastomosis of the tapered graft were at least twice as much as in the cylindrical graft, and the zones where these wall metrics reached high values corresponded to locations where NH formation is reported in literature. In addition, a comparison of the hemodynamic wall parameters at the two arterial anastomoses indicates that small flow rate increases the risk

of hemolysis in the tapered graft, whereas the cylindrical graft is completely free of hemolysis. Their results indicate that flow patterns played an important role in clinical studies in which tapered design grafts did not perform better when compared to the cylindrical design grafts.¹⁷

Sarmast *et al.*⁶⁷ investigated and compared the hemodynamics in two different sizes of hemodialysis AVG for upper arm VA, an 8 mm tapered to 6 mm at the arterial side and a straight 6 mm. They used CFD simulations, imposing physiological velocity and pressure waveforms as boundary conditions at the arterial inlet and venous outlet of the models, respectively, and then characterizing the disturbed flow by means of the spatial WSS gradient. The tapered graft was associated with less disturbed flow patterns within the venous anastomosis, but with the disadvantage of higher values of hemodynamic parameters at the arterial junction, attributable to its significantly higher mean blood flow rate. Their findings indicate that the tapered graft outperforms the straight one hemodynamically when used in upper arm hemodialysis VA.

Along the same line of research, Van Canneyt *et al.*⁷⁵ used CFD to investigate the impact of a helical graft design on the occurrence of favorable hemodynamic conditions at the venous anastomosis. Six models of prosthesis graft in a loop configuration were studied, one straight graft, and five helical grafts. At the venous anastomosis, disturbed shear, the bulk hemodynamics, and the pressure drop over the graft were assessed. The most helical design scored best, being instrumental in suppressing disturbed shear in the venous segment (Fig. 7). Bulk flow investigation showed a marked increase in helicity intensity and moderate pressure drop over the AVG by introducing a lower pitch.

In a similar study, Kabinejadian *et al.*³⁶ investigated, with CFD, the utility of a coupled, sequential *side-to-side* followed by an *end-to-side* venous anastomotic (CSQA) design, compared to the conventional, *end-to-side-only* venous anastomosis in AVG for hemodialysis. Two complete AVG idealized models with the proposed and the conventional venous anastomosis configurations were generated, assuming the diameter of the artery to be 4, that of the vein 6, and of the graft 6 mm, with a graft length of 30 cm, and an anastomotic angle of 30° in both models. Pulsatile blood flow through the models was simulated and hemodynamic wall parameters (TAWSS, TAWSSG, OSI and RRT) were compared in the two models. Simulation results demonstrated that the proposed anastomotic design provides a more uniform and smooth flow at the *end-to-side* anastomosis, without flow impingement and a stagnation point on the artery bed and vortex formation in the heel region, a more

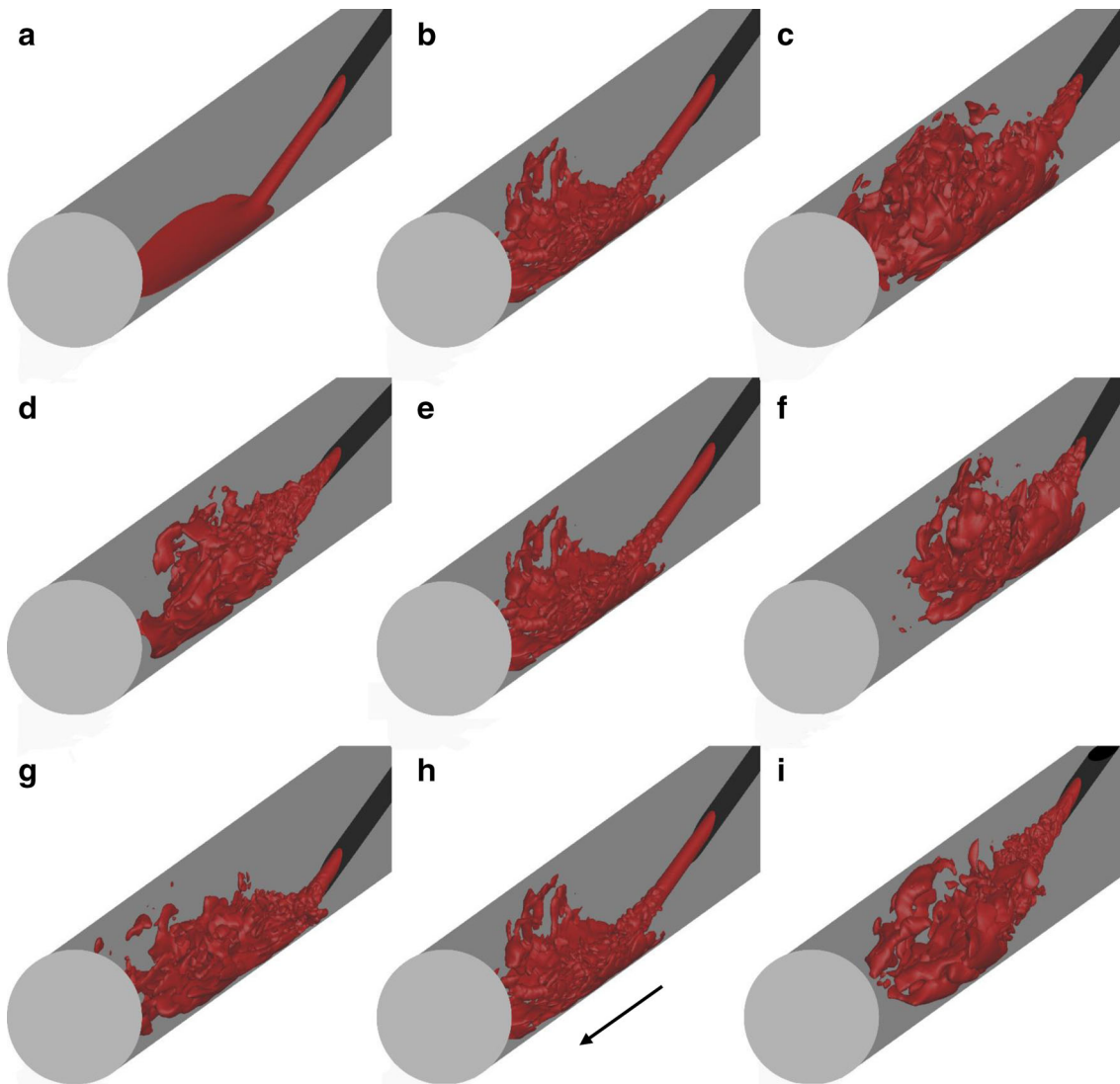


FIGURE 10. Velocity iso-surfaces (1 m/s) visualizing the venous needle jet. (a)–(c) Variation in blood flow rate (200, 300, and 400 mL/min). (d)–(f) Variation in needle angle (10°, 20°, 30°). (g)–(i) Variation in needle position (bottom, central, top). The arrow indicate the direction of bulk blood flow. Reprinted by permission from ASME.²⁶

uniform distribution of WSS and substantially lower WSS gradients on the venous wall (Fig. 8). Their design has advantages that might improve the hemodynamic environment towards enhancing the patency of AVG for hemodialysis.

Cannulation Needles

Cannulation to withdraw or to return blood to and from the vasculature may directly affect the maintenance and patency of the VA. Co-morbidities related to repeated cannulation may be stenosis, hematoma, infection, and aneurysm formation.⁷⁷

The cannulation must be performed on a usable vein tract of the VA that is as straight as possible, as shown schematically in Fig. 9. Here, the arterial needle

is used to withdraw blood from the vasculature to the extracorporeal circuit and may be inserted either in the same direction of blood flow (antegrade) or in the opposite direction (retrograde). The venous needle is used to return the blood from the dialysis machine to the body and must always point in the antegrade direction. Guidelines for the cannulation procedure focus on needle size, the angle of needle insertion, the direction of the needle bevel, and the rotation of needles after insertion.⁵⁹ The needle should always be inserted with the bevel facing upward and then rotated 180° (“flipping”) around its axis to prevent posterior wall infiltration, which can occur if the needle’s bevel tip accidentally punctures the bottom of the graft or fistula. Arterial needles with a back-eye, as recommended by guidelines,⁵⁷ may alleviate the high pressure

present at the central bore and reduce the need for flipping.⁵⁹ Since the venous needle produces turbulent flow⁷³ and turbulent stresses from the needle jet that reach the venous wall may contribute to EC dysfunction,³² this particular hemodynamic condition of VA is worth investigating.

Fulker *et al.*²⁵ studied the flow field in the region of the venous needle computationally. Four scenarios were simulated by varying the needle placement angle, the blood flow rate, the needle depth (top, middle, bottom), and the presence or absence of a back-eye in the needle design. The presence of the needle had a significant effect on the flow field, with the different scenarios having varying influence. In general, WSS were elevated above normal physiological values, and there was an increased presence of areas of low velocity and recirculation, indicating increased likelihood of NH development. Their initial findings indicated that narrow needle angles and lower blood flow rates might minimize the vessel damage. The same group²⁷ followed this line of research by analyzing the hemodynamic effects of needle rotation and orientation in an idealized model of the cephalic vein. The hemodynamic benefits were investigated in terms of TAWSS and disturbed flow (OSI) patterns. They simulated 180° rotation (“flipping”) of the needle around its axis, done to prevent posterior wall infiltration, which can occur if the needle’s bevel tip accidentally punctures the bottom of the graft or fistula. The CFD study was conducted with antegrade and retrograde orientations of the arterial needle, whereas the venous needle was kept in the antegrade orientation. In each case, arterial needle rotation offered no hemodynamic benefit in minimizing the conditions known to cause endothelial damage, whereas the venous needle rotation reduced the maximum hemodynamic shear. They concluded that both needles may be rotated, while the arterial needle in antegrade orientation produced a larger region of oscillatory shear compared to retrograde orientation. The same authors²⁶ studied the hemodynamic environment in the vicinity of the arterial and venous needle during the HD session in an idealized model of the outflow vein from a radial-cephalic AVF, using HR CFD. Disturbed flow, localized using high RRT, was found around the arterial needle tip in either an antegrade or retrograde orientation, resulting from near-wall regions with low velocity and high residency time on the surface of the vein, a condition that may impair endothelial function. On the contrary, a high speed jet exits the venous needle, producing high WSS at the point of impingement, which can injure the endothelium (Fig. 10). The secondary flows produced by jet dissipation also resulted in regions of high residency time, which may influence endothelial structure, leading to NH. They concluded

by recommending using shallow needle angles, a blood flow rate of approximately 300 mL/min and keeping the needle tip away from the walls of the vein to mitigate the risks of NH.

Modular Anastomotic Valve Devices

Motivated by evidence that flow disturbances promote NH formation, McNally *et al.*⁵² designed a modular anastomotic valve device (MAVD) capable of isolating the graft from the circulation between dialysis periods (closed position) and enabling VA during dialysis (open position). The objective of their preliminary CFD study was to assess the device’s ability to normalize venous flow between dialysis. A computational study was performed in a cylindrical tube resembling the native vein, with two MAVD having anastomotic angles of 90° and 30°. Regions prone to NH development were characterized in terms of hemodynamic wall metrics. The closed MAVD had similar flow characteristics as the native vein, with very low differences (0.3% difference in pressure drop, 3.5% difference in surface TAWSS). The open MAVD generated five disturbed flow regions, exhibiting different degrees of flow reversal (surface-averaged OSI between 0.03 and 0.36) and stagnation (max RRT between 2.50 and 37.16). The reduction of anastomotic angle resulted in the suppression of three disturbed flow regions and overall reductions in flow reversal (surface-averaged OSI < 0.21) and stagnation (max RRT < 18.05). Their study showed the ability of the MAVD to normalize venous flow between dialysis periods while generating the typical hemodynamics of *end-to-side* vein graft anastomoses during dialysis.

DISCUSSION

Numerical modelling on idealized geometries was widely used in cardiovascular biomechanics research to assess the flow field in studying the link between hemodynamics and cardiovascular disease. This kind of approach may seem over simplistic, but experimental fluid mechanics phenomena^{1,2} and numerical validation in three-dimensional idealized models^{28,69} of complex fluid mechanics phenomena are good practice before tackling to patient-specific simulations.^{43,45} Such studies help to better understand the hemodynamic capturing the essential features of real flow, providing, at the same time, a simpler framework for studying the effect of different geometrical aspects and flow ranges on local hemodynamics. Despite its clinical relevance, this type of investigational method was used less in the study of VA complications: in relation to the literature on carotid bifurcation or coronary arteries,

there were relatively few papers that addressed this task by means of numerical modelling.

In this literature review we summarized the knowledge gained with in computational studies in idealized models in the VA research. Most of them were published starting with the last decade (Table 1). On the one hand, the findings of computational studies in idealized models of VA highlighted that numerical modelling, especially HR-CFD, is valuable in assessing the flow phenotype, especially in view of the high blood volume flow rates that develop after the surgical creation of VA. The findings of such studies proved very helpful for basic research into AVF and AVG complications. Many of the successes achieved in current VA applications originated from these idealized model studies, including the role of disturbed flow in NH, the detrimental role of turbulent flow, the beneficial role of spiral flow, improvements in 0D-1D models of arm vasculature, and the study of needle insertion hemodynamics.

In the two DNS studies on AVG,^{46,48} high velocity and pressure fluctuations were observed for the 70:30 and 85:15 split ratio (PV:DV) cases and absent in the 100:0 and 115:(15) cases. Similarly, in a LES approach,⁹ the flow split ratio, more than the Reynolds number, had the largest influence on turbulence generation in the vein. Therefore, in AVG one potential clinical application of such findings might be to close off the distal vein during graft construction to ensure a 100:0 flow division. This may also suggest a potential hemodynamic advantage of the *end-to-end* over the *side-to-end* or *end-to-side* anastomoses design. Unfortunately, in *side-to-end* AVF the flow in DA depends on the overall resistance of the shunt and cannot be influenced at the time of VA surgery.

From the computational simulation point of view, the use of the tapered hemodialysis grafts proved to be somewhat controversial. While some studies demonstrated less disturbed flow patterns within the venous anastomosis than were observed in the tapered grafts,⁶⁷ other simulations indicated that the tapered arteriovenous grafts did not show better outcomes.⁷⁸ Regarding the study of helical design AVG, Van Canneyt *et al.*⁷⁵ concluded that there are no trivial relationships between the number of helix turns of the graft and disturbed shear in the venous segment, when a realistic closed-loop AVG model is investigated. However, due to the complex flow conditions, the optimal helical design for an AVG cannot be derived without studying it case by case.

An important issue for computational studies is the dimensional aspect of idealized models used in the CFD simulations. It is not clear why Iori *et al.*³³ used a vein diameter smaller than that of the artery, since the

diameter of the vein is usually higher.¹⁵ Either way, even though their results might not be influenced by the diameter of the vein, their two recommendations seem incompatible, highlighting the importance of ascertaining the exact mechanisms that cause NH in the VA. Nonetheless, their results illustrate the important role played by the arterial curvature in determining AVF hemodynamics, which has been overlooked in previous studies.

Among limitations, in nearly all of the reviewed studies there is also the lack of compliance of the VA wall, with only the work of Ngoepe *et al.*⁵⁵ being specifically designed to assess fluid and structural anastomotic mechanics. This issue could be addressed in future studies by conducting fluid–solid interaction (FSI) analysis, although two patient-specific^{19,51} showed that rigid-wall hemodynamic simulations can predict blood hemodynamics within the same order of accuracy of the FSI equivalent simulations in patient-specific AVF. Moreover, a concrete suggestion is that a full FSI study is not always needed since the vessel wall deformability has limited influence on blood flow dynamics, the higher computational making its clinical use challenging.¹⁹

The initial study by Fulker *et al.*²⁵ indicated that the presence of the venous needle in a hemodialysis fistula may lead to abnormal wall shear stress. In fact, Unnikrishnan *et al.* found, experimentally,⁷³ that there is considerably higher turbulence downstream of the venous needle, compared with graft flow alone. The turbulent fluctuations downstream peaked at 2 cm, and persisted down to nearly 7 cm from the tip of the needle. These findings were further confirmed by the same group³² in an *in vitro* study showing that EC lose their alignment and have decreased NO production in the presence of needle flow. Thus, the turbulent flow caused by the needle *jet alone* may contribute to the cascade of events leading to NH formation during hemodialysis. As hemodialysis patients are exposed to needle turbulence for about 4 h, three times a week, the role of postvenous needle turbulence may be important in the pathogenesis of VA complications. Another important aspect is the *site* of puncture location, because if the needle is placed 4–5 cm from the anastomosis then the needle-induced turbulent fluctuations may overlay those regularly developed in the VA downstream from the venous anastomosis. Fulker *et al.*²⁷ further showed that the arterial needle in the antegrade orientation produces a larger region of oscillatory shear compared to the retrograde orientation. Although either antegrade or retrograde arterial needle placement were shown to perform similarly in terms of HD adequacy,⁵⁸ long-term outcomes of the arterial needle placement such as stenosis and thrombosis of the VA warrant further studies.

Recommendations and Future Directions

This review highlighted that computational studies in *idealized* models are essential for studying the overall and local blood flow features in VA for hemodialysis. To this end, the VA research must parallel achievements in all research fields and be up-to-date in terms of numerical technology and novel hemodynamic concepts. We strongly recommend several *good practice rules* for guiding future computational studies in idealized, as well as in patient-specific VA.

Proper Dimensional Setting of the Model and Boundary Conditions

It is notable that in normally operating VA, vessel diameter and blood flow rate have a steep increase in the first day,¹⁵ and then have a linear-asymptotic increase for up to one year of follow-up.^{18,22} The proper modelling should thus take into account the realistic dimensions of vascular anastomoses and the blood flow rates and split ratio encountered in hemodialysis VA at the *time of analysis*.

Adequate Mesh Resolution

Following a good dimensional setting, a fine numerical grid should be generated for CFD. Mesh resolution and estimation of discretization of numerical uncertainties are standardized by the GCI method based on Richardson extrapolation.¹³ In VA research there are examples of applying this method either in idealized¹² or patient-specific⁷ AVF models.

Numerical Approach Tweaked to Catch Flow Turbulence

The high blood flow in the VA is transitional from laminar to turbulent, requiring using properly set HR-CFD.³⁸ Good results were obtained with many of the commercial or open-source CFD packages available today (Table 1). We also emphasize the need for future DNS studies to elucidate whether the HR-CFD simulations perform well when detecting the flow phenotypes in VA for hemodialysis.

Postprocessing of Results with Focus on Validated Metrics

The high-frequency flow instabilities developing, particularly in the venous segment of VA, require using bulk flow estimation specific to turbulent flows, including turbulent kinetic energy and hemodynamic wall metrics that take into account the disturbances of the WSS vector at the sites of higher turbulence. The hemodynamic vascular wall metric transWSS^{53,54} was

proven to accurate also in VA,^{7,24} as well as in the aorta where similar turbulent regimes develop.⁵

CONCLUSIONS

The numerical technologies available today may help us to understand the underlying mechanisms of NH, as well as optimizing AVF shape or designing AVG and dialysis needles. In an effort to scrutinize current knowledge about the role of hemodynamics in *idealized* VA, our review highlighted inhomogeneity between studies. These findings emphasize the need for a unified hypothesis and standard numerical and postprocessing techniques. From a clinical point of view, our results further reinforce the need for longitudinal studies to comprehensively evaluate the relationship between shear stress and NH formation failure.^{10,16} To achieve the best results, the physics of blood behavior inside the VA for hemodialysis should be modeled correctly, and its interactions with the vessel wall assessed properly.

ACKNOWLEDGMENTS

The authors would like to thank Kerstin Mierke for editorial assistance during preparation of the manuscript.

CONFLICT OF INTEREST

BE-I and AR declare that they have no conflict of interest.

ETHICAL APPROVAL

This article does not contain any studies with human participants or animals performed by any of the authors.

REFERENCES

- ¹Ahmed, S. A., and D. P. Giddens. Flow disturbance measurements through a constricted tube at moderate Reynolds numbers. *J. Biomech.* 16(12):955–963, 1983.
- ²Ahmed, S. A., and D. P. Giddens. Pulsatile poststenotic flow studies with laser Doppler anemometry. *J. Biomech.* 17(9):695–705, 1984.
- ³Al-Jaishi, A. A., M. J. Oliver, S. M. Thomas, C. E. Lok, J. C. Zhang, A. X. Garg, *et al.* Patency rates of the arteriovenous fistula for hemodialysis: a systematic review and

- meta-analysis. *Am. J. Kidney Dis.* 63(3):464–478, 2014. doi:[10.1053/j.ajkd.2013.08.023](https://doi.org/10.1053/j.ajkd.2013.08.023).
- ⁴Allon, M., and M. L. Robbin. Increasing arteriovenous fistulas in hemodialysis patients: problems and solutions. *Kidney Int.* 62(4):1109–1124, 2002.
- ⁵Andersson, M., J. Lantz, T. Ebberts, and M. Karlsson. Multidirectional WSS disturbances in stenotic turbulent flows: a pre- and post-intervention study in an aortic coarctation. *J. Biomech.* 2016. doi:[10.1016/j.jbiomech.2016.11.064](https://doi.org/10.1016/j.jbiomech.2016.11.064).
- ⁶Badero, O. J., M. O. Salifu, H. Wasse, and J. Work. Frequency of swing-segment stenosis in referred dialysis patients with angiographically documented lesions. *Am. J. Kidney Dis.* 51(1):93–98, 2008. doi:[10.1053/j.ajkd.2007.09.012](https://doi.org/10.1053/j.ajkd.2007.09.012).
- ⁷Bozzetto, M., B. Ene-Iordache, and A. Remuzzi. Transitional flow in the venous side of patient-specific arteriovenous fistulae for hemodialysis. *Ann. Biomed. Eng.* 44(8):2388–2401, 2016. doi:[10.1007/s10439-015-1525-y](https://doi.org/10.1007/s10439-015-1525-y).
- ⁸Brescia, M. J., J. E. Cimino, K. Appel, and B. J. Hurwicz. Chronic hemodialysis using venipuncture and a surgically created arteriovenous fistula. *N. Engl. J. Med.* 275(20):1089–1092, 1966.
- ⁹Broderick, S. P., J. G. Houston, and M. T. Walsh. The influence of the instabilities in modelling arteriovenous junction haemodynamics. *J. Biomech.* 48(13):3591–3598, 2015. doi:[10.1016/j.jbiomech.2015.07.038](https://doi.org/10.1016/j.jbiomech.2015.07.038).
- ¹⁰Browne, L. D., K. Bashar, P. Griffin, E. G. Kavanagh, S. R. Walsh, and M. T. Walsh. The role of shear stress in arteriovenous fistula maturation and failure: a systematic review. *PLoS ONE* 10(12):e0145795, 2015. doi:[10.1371/journal.pone.0145795](https://doi.org/10.1371/journal.pone.0145795).
- ¹¹Browne, L. D., P. Griffin, K. Bashar, S. R. Walsh, E. G. Kavanagh, and M. T. Walsh. In vivo validation of the in silico predicted pressure drop across an arteriovenous fistula. *Ann. Biomed. Eng.* 43(6):1275–1286, 2015. doi:[10.1007/s10439-015-1295-6](https://doi.org/10.1007/s10439-015-1295-6).
- ¹²Browne, L. D., M. T. Walsh, and P. Griffin. Experimental and numerical analysis of the bulk flow parameters within an arteriovenous fistula. *Cardiovasc. Eng. Technol.* 6(4):450–462, 2015. doi:[10.1007/s13239-015-0246-6](https://doi.org/10.1007/s13239-015-0246-6).
- ¹³Celik, I. B., U. Ghia, P. J. Roache, C. J. Freitas, H. Coleman, and P. E. Raad. Procedure for estimation and reporting of uncertainty due to discretization in CFD applications. *J. Fluids Eng.* 130:1–4, 2008.
- ¹⁴Chiu, J. J., and S. Chien. Effects of disturbed flow on vascular endothelium: pathophysiological basis and clinical perspectives. *Physiol. Rev.* 91(1):327–387, 2011. doi:[10.1152/physrev.00047.2009](https://doi.org/10.1152/physrev.00047.2009).
- ¹⁵Corpataux, J. M., E. Haesler, P. Silacci, H. B. Ris, and D. Hayoz. Low-pressure environment and remodelling of the forearm vein in Brescia-Cimino haemodialysis access. *Nephrol. Dial. Transpl.* 17(6):1057–1062, 2002.
- ¹⁶Cunnane, C. V., E. M. Cunnane, and M. T. Walsh. A review of the hemodynamic factors believed to contribute to vascular access dysfunction. *Cardiovasc. Eng. Technol.* 2017. doi:[10.1007/s13239-017-0307-0](https://doi.org/10.1007/s13239-017-0307-0).
- ¹⁷Dammers, R., R. N. Planken, K. P. Pouls, R. J. Van Det, H. Burger, F. M. Van Der Sande, et al. Evaluation of 4-mm to 7-mm versus 6-mm prosthetic brachial-antecubital forearm loop access for hemodialysis: results of a randomized multicenter clinical trial. *J. Vasc. Surg.* 37(1):143–148, 2003.
- ¹⁸Dammers, R., J. H. Tordoir, J. P. Kooman, R. J. Welten, J. M. Hameleers, P. J. Kitslaar, et al. The effect of flow changes on the arterial system proximal to an arteriovenous fistula for hemodialysis. *Ultrasound Med. Biol.* 31(10):1327–1333, 2005.
- ¹⁹Decorato, I., Z. Kharboutly, T. Vassallo, J. Penrose, C. Legallais, and A. V. Salsac. Numerical simulation of the fluid structure interactions in a compliant patient-specific arteriovenous fistula. *Int. J. Numer. Method Biomed. Eng.* 30(2):143–159, 2014. doi:[10.1002/cnm.2595](https://doi.org/10.1002/cnm.2595).
- ²⁰Ene-Iordache, B. Haemodynamics and vascular remodeling in vascular access: insights from numerical studies [Doctoral dissertation]. Eindhoven: Technische Universiteit Eindhoven, 2015.
- ²¹Ene-Iordache, B., L. Cattaneo, G. Dubini, and A. Remuzzi. Effect of anastomosis angle on the localization of disturbed flow in ‘side-to-end’ fistulae for haemodialysis access. *Nephrol. Dial. Transpl.* 28(4):997–1005, 2013. doi:[10.1093/ndt/gfs298](https://doi.org/10.1093/ndt/gfs298).
- ²²Ene-Iordache, B., L. Mosconi, L. Antiga, S. Bruno, A. Anghileri, G. Remuzzi, et al. Radial artery remodeling in response to shear stress increase within arteriovenous fistula for hemodialysis access. *Endothelium* 10(2):95–102, 2003.
- ²³Ene-Iordache, B., and A. Remuzzi. Disturbed flow in radial-cephalic arteriovenous fistulae for haemodialysis: low and oscillating shear stress locates the sites of stenosis. *Nephrol. Dial. Transpl.* 27(1):358–368, 2012. doi:[10.1093/ndt/gfr342](https://doi.org/10.1093/ndt/gfr342).
- ²⁴Ene-Iordache, B., C. Semperboni, G. Dubini, and A. Remuzzi. Disturbed flow in a patient-specific arteriovenous fistula for hemodialysis: multidirectional and reciprocating near-wall flow patterns. *J. Biomech.* 2015. doi:[10.1016/j.jbiomech.2015.04.013](https://doi.org/10.1016/j.jbiomech.2015.04.013).
- ²⁵Fulker, D., M. Kang, A. Simmons, and T. Barber. The flow field near a venous needle in hemodialysis: a computational study. *Hemodial. Int.* 17(4):602–611, 2013. doi:[10.1111/hdi.12029](https://doi.org/10.1111/hdi.12029).
- ²⁶Fulker, D., A. Simmons, and T. Barber. Computational model of the arterial and venous needle during haemodialysis. *J. Biomech. Eng.* 2017. doi:[10.1115/1.4034429](https://doi.org/10.1115/1.4034429).
- ²⁷Fulker, D., A. Simmons, K. Kabir, L. Kark, and T. Barber. The hemodynamic effects of hemodialysis needle rotation and orientation in an idealized computational model. *Artif. Organs* 40(2):185–189, 2016. doi:[10.1111/aor.12521](https://doi.org/10.1111/aor.12521).
- ²⁸Gardhagen, R., J. Lantz, F. Carlsson, and M. Karlsson. Quantifying turbulent wall shear stress in a stenosed pipe using large eddy simulation. *J. Biomech. Eng.* 132(6):061002, 2010. doi:[10.1115/1.4001075](https://doi.org/10.1115/1.4001075).
- ²⁹Himburg, H. A., and M. H. Friedman. Correspondence of low mean shear and high harmonic content in the porcine iliac arteries. *J. Biomech. Eng.* 128(6):852–856, 2006. doi:[10.1115/1.2354211](https://doi.org/10.1115/1.2354211).
- ³⁰Hoganson, D. M., C. J. Hinkel, X. Chen, R. K. Agarwal, and S. Shenoy. Validation of computational fluid dynamics-based analysis to evaluate hemodynamic significance of access stenosis. *J. Vasc. Access.* 15(5):409–414, 2014. doi:[10.5301/jva.5000226](https://doi.org/10.5301/jva.5000226).
- ³¹Hull, J. E., B. V. Balakin, B. M. Kellerman, and D. K. Wrolstad. Computational fluid dynamic evaluation of the side-to-side anastomosis for arteriovenous fistula. *J. Vasc. Surg.* 58(1):187–93.e1, 2013. doi:[10.1016/j.jvs.2012.10.070](https://doi.org/10.1016/j.jvs.2012.10.070).
- ³²Huynh, T. N., B. K. Chacko, X. Teng, B. C. Brott, M. Allon, S. S. Kelpke, et al. Effects of venous needle turbulence during ex vivo hemodialysis on endothelial morphology and nitric oxide formation. *J. Biomech.* 40(10):2158–2166, 2007. doi:[10.1016/j.jbiomech.2006.10.028](https://doi.org/10.1016/j.jbiomech.2006.10.028).

- ³³Iori, F., L. Grechy, R. W. Corbett, W. Gedroyc, N. Duncan, C. G. Caro, *et al.* The effect of in-plane arterial curvature on blood flow and oxygen transport in arteriovenous fistulae. *Phys. Fluids* 27(3):031903, 2015. doi:10.1063/1.4913754.
- ³⁴Jennings, W. C. Creating arteriovenous fistulas in 132 consecutive patients: exploiting the proximal radial artery arteriovenous fistula: reliable, safe, and simple forearm and upper arm hemodialysis access. *Arch. Surg.* 141(1):32, 2006. doi:10.1001/archsurg.141.1.27.
- ³⁵Jia, L., L. Wang, F. Wei, H. Yu, H. Dong, B. Wang, *et al.* Effects of wall shear stress in venous neointimal hyperplasia of arteriovenous fistulae. *Nephrology*. 20(5):335–342, 2015. doi:10.1111/nep.12394.
- ³⁶Kabinejadian, F., B. Su, D. N. Ghista, M. Ismail, S. Kim, and H. L. Leo. Sequential venous anastomosis design to enhance patency of arterio-venous grafts for hemodialysis. *Comput. Methods Biomech. Biomed. Eng.* 2016. doi:10.1080/10255842.2016.1200564.
- ³⁷Kanterman, R. Y., T. M. Vesely, T. K. Pilgram, B. W. Guy, D. W. Windus, and D. Picus. Dialysis access grafts: anatomic location of venous stenosis and results of angioplasty. *Radiology* 195:135–139, 1995.
- ³⁸Khan, M. O., K. Valen-Sendstad, and D. A. Steinman. Narrowing the expertise gap for predicting intracranial aneurysm hemodynamics: impact of solver numerics versus mesh and time-step resolution. *AJNR Am. J. Neuroradiol.* 36(7):1310–1316, 2015. doi:10.3174/ajnr.A4263.
- ³⁹Konner, K. The anastomosis of the arteriovenous fistula—common errors and their avoidance. *Nephrol. Dial. Transpl.* 17(3):376–379, 2002.
- ⁴⁰Konner, K. The initial creation of native arteriovenous fistulas: surgical aspects and their impact on the practice of nephrology. *Semin. Dial.* 16(4):291–298, 2003.
- ⁴¹Krishnamoorthy, M., P. Roy-Chaudhury, Y. Wang, A. Sinha Roy, J. Zhang, S. Khoury, *et al.* Measurement of hemodynamic and anatomic parameters in a swine arteriovenous fistula model. *J. Vasc. Access.* 9(1):28–34, 2008.
- ⁴²Krueger, U., J. Zanow, and H. Scholz. Computational fluid dynamics and vascular access. *Artif. Organs* 26(7):571–575, 2002.
- ⁴³Lantz, J., T. Ebberts, J. Engvall, and M. Karlsson. Numerical and experimental assessment of turbulent kinetic energy in an aortic coarctation. *J. Biomech.* 46(11):1851–1858, 2013. doi:10.1016/j.jbiomech.2013.04.028.
- ⁴⁴Lee, S. W., L. Antiga, and D. A. Steinman. Correlations among indicators of disturbed flow at the normal carotid bifurcation. *J. Biomech. Eng.* 131(6):061013, 2009.
- ⁴⁵Lee, S. E., S. W. Lee, P. F. Fischer, H. S. Bassiouny, and F. Loth. Direct numerical simulation of transitional flow in a stenosed carotid bifurcation. *J. Biomech.* 41(11):2551–2561, 2008. doi:10.1016/j.jbiomech.2008.03.038.
- ⁴⁶Lee, S. W., D. S. Smith, F. Loth, P. F. Fischer, and H. S. Bassiouny. Importance of flow division on transition to turbulence within an arteriovenous graft. *J. Biomech.* 40(5):981–992, 2007. doi:10.1016/j.jbiomech.2006.03.024.
- ⁴⁷Leschziner, M. *Statistical Turbulence Modelling for Fluid Dynamics Demystified: An Introductory Text for Graduate Engineering Students*. London: Imperial College Press, 2015.
- ⁴⁸Loth, F., P. F. Fischer, N. Arslan, C. D. Bertram, S. E. Lee, T. J. Royston, *et al.* Transitional flow at the venous anastomosis of an arteriovenous graft: potential activation of the ERK1/2 mechanotransduction pathway. *J. Biomech. Eng.* 125(1):49–61, 2003.
- ⁴⁹Lu, D. Y., E. Y. Chen, D. J. Wong, K. Yamamoto, C. D. Protack, W. T. Williams, *et al.* Vein graft adaptation and fistula maturation in the arterial environment. *J. Surg. Res.* 188(1):162–173, 2014. doi:10.1016/j.jss.2014.01.042.
- ⁵⁰MacRae, J. M. Vascular access and cardiac disease: is there a relationship? *Curr. Opin. Nephrol. Hypertens.* 15(6):577–582, 2006.
- ⁵¹McGah, P. M., D. F. Leotta, K. W. Beach, and A. Aliseda. Effects of wall distensibility in hemodynamic simulations of an arteriovenous fistula. *Biomech. Model. Mechanobiol.* 13(3):679–695, 2014. doi:10.1007/s10237-013-0527-7.
- ⁵²McNally, A., A. G. Akingba, E. A. Robinson, and P. Suscosky. Novel modular anastomotic valve device for hemodialysis vascular access: preliminary computational hemodynamic assessment. *J. Vasc. Access.* 15(6):448–460, 2014. doi:10.5301/jva.5000284.
- ⁵³Mohamied, Y., E. M. Rowland, E. L. Bailey, S. J. Sherwin, M. A. Schwartz, and P. D. Weinberg. Change of direction in the biomechanics of atherosclerosis. *Ann. Biomed. Eng.* 43(1):16–25, 2015. doi:10.1007/s10439-014-1095-4.
- ⁵⁴Mohamied, Y., S. J. Sherwin, and P. D. Weinberg. Understanding the fluid mechanics behind transverse wall shear stress. *J. Biomech.* 2016. doi:10.1016/j.jbiomech.2016.11.035.
- ⁵⁵Ngoepe, M. N., B. D. Reddy, D. C. M. Kahn, and P. T. F. Zilla. A numerical tool for the coupled mechanical assessment of anastomoses of PTFE arterio-venous access grafts. *Cardiovasc. Eng. Technol.* 2(3):160–172, 2011.
- ⁵⁶Niemann, A. K., J. Udesen, S. Thrysoe, J. V. Nygaard, E. T. Frund, S. E. Petersen, *et al.* Can sites prone to flow induced vascular complications in a-v fistulas be assessed using computational fluid dynamics? *J. Biomech.* 43(10):2002–2009, 2010.
- ⁵⁷NKF/KDOQI. Clinical practice guidelines for vascular access. Update 2006.
- ⁵⁸Ozmen, S., A. K. Kadiroglu, C. A. Ozmen, R. Danis, D. Sit, D. Akin, *et al.* Does the direction of arterial needle in AV fistula cannulation affect dialysis adequacy? *Clin. Nephrol.* 70(3):229–232, 2008.
- ⁵⁹Parisotto, M. T., V. U. Schoder, C. Miriunis, A. H. Grassmann, L. P. Scatizzi, P. Kaufmann, *et al.* Cannulation technique influences arteriovenous fistula and graft survival. *Kidney Int.* 86(4):790–797, 2014. doi:10.1038/ki.2014.96.
- ⁶⁰Peiffer, V., S. J. Sherwin, and P. D. Weinberg. Computation in the rabbit aorta of a new metric—the transverse wall shear stress—to quantify the multidirectional character of disturbed blood flow. *J. Biomech.* 46(15):2651–2658, 2013. doi:10.1016/j.jbiomech.2013.08.003.
- ⁶¹Potter, C. M., M. H. Lundberg, L. S. Harrington, C. M. Warboys, T. D. Warner, R. E. Berson, *et al.* Role of shear stress in endothelial cell morphology and expression of cyclooxygenase isoforms. *Arterioscler. Thromb. Vasc. Biol.* 31(2):384–391, 2011. doi:10.1161/ATVBAHA.110.214031.
- ⁶²Quencer, K. B., and M. Arici. Arteriovenous fistulas and their characteristic sites of stenosis. *AJR Am. J. Roentgenol.* 205(4):726–734, 2015. doi:10.2214/AJR.15.14650.
- ⁶³Rajabi-Jagahrgh, E., M. K. Krishnamoorthy, P. Roy-Chaudhury, P. Succop, Y. Wang, A. Choe, *et al.* Longitudinal assessment of hemodynamic endpoints in predicting arteriovenous fistula maturation. *Semin. Dial.* 26(2):208–215, 2013. doi:10.1111/j.1525-139X.2012.01112.x.
- ⁶⁴Rajabi-Jagahrgh, E., M. K. Krishnamoorthy, Y. Wang, A. Choe, P. Roy-Chaudhury, and R. K. Banerjee. Influence of temporal variation in wall shear stress on intima-media thickening in arteriovenous fistulae. *Semin. Dial.* 26(4):511–519, 2013. doi:10.1111/sdi.12045.

- ⁶⁵Roy-Chaudhury, P., L. Arend, J. Zhang, M. Krishnamoorthy, Y. Wang, R. Banerjee, *et al.* Neointimal hyperplasia in early arteriovenous fistula failure. *Am. J. Kidney Dis.* 50(5):782–790, 2007.
- ⁶⁶Roy-Chaudhury, P., V. P. Sukhatme, and A. K. Cheung. Hemodialysis vascular access dysfunction: a cellular and molecular viewpoint. *J. Am. Soc. Nephrol.* 17(4):1112–1127, 2006.
- ⁶⁷Sarmast, M., H. Niroomand-Oscuii, F. Ghalichi, and E. Samiei. Evaluation of the hemodynamics in straight 6-mm and tapered 6- to 8-mm grafts as upper arm hemodialysis vascular access. *Med. Biol. Eng. Comput.* 52(9):797–811, 2014. doi:[10.1007/s11517-014-1181-7](https://doi.org/10.1007/s11517-014-1181-7).
- ⁶⁸Scheltinga, M. R., and C. M. Bruijninckx. Haemodialysis access-induced distal ischaemia (HAIDI) is caused by loco-regional hypotension but not by steal. *Eur. J. Vasc. Endovasc. Surg.* 43(2):218–223, 2012. doi:[10.1016/j.ejvs.2011.10.018](https://doi.org/10.1016/j.ejvs.2011.10.018).
- ⁶⁹Sherwin, S. J., and H. M. Blackburn. Three-dimensional instabilities and transition of steady and pulsatile axisymmetric stenotic flows. *J. Fluid Mech.* 533:297–327, 2005.
- ⁷⁰Sivanesan, S., T. V. How, and A. Bakran. Characterizing flow distributions in AV fistulae for haemodialysis access. *Nephrol. Dial. Transpl.* 13(12):3108–3110, 1998.
- ⁷¹Sivanesan, S., T. V. How, and A. Bakran. Sites of stenosis in AV fistulae for haemodialysis access. *Nephrol. Dial. Transpl.* 14(1):118–120, 1999.
- ⁷²Tordoir, J., B. Canaud, P. Haage, K. Konner, A. Basci, D. Fouque, *et al.* EBPG on vascular access. *Nephrol. Dial. Transpl.* 22(Suppl 2):88–117, 2007.
- ⁷³Unnikrishnan, S., T. N. Huynh, B. C. Brott, Y. Ito, C. H. Cheng, A. M. Shih, *et al.* Turbulent flow evaluation of the venous needle during hemodialysis. *J. Biomech. Eng.* 127(7):1141–1146, 2005.
- ⁷⁴Valen-Sendstad, K., M. Piccinelli, and D. A. Steinman. High-resolution computational fluid dynamics detects flow instabilities in the carotid siphon: implications for aneurysm initiation and rupture? *J. Biomech.* 47(12):3210–3216, 2014. doi:[10.1016/j.jbiomech.2014.04.018](https://doi.org/10.1016/j.jbiomech.2014.04.018).
- ⁷⁵Van Canneyt, K., U. Morbiducci, S. Eloot, G. De Santis, P. Segers, and P. Verdonck. A computational exploration of helical arterio-venous graft designs. *J. Biomech.* 46(2):345–353, 2013. doi:[10.1016/j.jbiomech.2012.10.027](https://doi.org/10.1016/j.jbiomech.2012.10.027).
- ⁷⁶Van Canneyt, K., T. Pourchez, S. Eloot, C. Guillame, A. Bonnet, P. Segers, *et al.* Hemodynamic impact of anastomosis size and angle in side-to-end arteriovenous fistulae: a computer analysis. *J. Vasc. Access.* 11(1):52–58, 2010.
- ⁷⁷van Loon, M. M., A. G. Kessels, F. M. Van der Sande, and J. H. Tordoir. Cannulation and vascular access-related complications in hemodialysis: factors determining successful cannulation. *Hemodial. Int.* 13(4):498–504, 2009. doi:[10.1111/j.1542-4758.2009.00382.x](https://doi.org/10.1111/j.1542-4758.2009.00382.x).
- ⁷⁸Van Tricht, I., D. De Wachter, J. Tordoir, and P. Verdonck. Comparison of the hemodynamics in 6 mm and 4–7 mm hemodialysis grafts by means of CFD. *J. Biomech.* 39(2):226–236, 2006.
- ⁷⁹Vassalotti, J. A., W. C. Jennings, G. A. Beathard, M. Neumann, S. Caponi, C. H. Fox, *et al.* Fistula first breakthrough initiative: targeting catheter last in fistula first. *Semin. Dial.* 25(3):303–310, 2012. doi:[10.1111/j.1525-139X.2012.01069.x](https://doi.org/10.1111/j.1525-139X.2012.01069.x).
- ⁸⁰Wang, C., B. M. Baker, C. S. Chen, and M. A. Schwartz. Endothelial cell sensing of flow direction. *Arterioscler. Thromb. Vasc. Biol.* 33(9):2130–2136, 2013. doi:[10.1161/ATVBAHA.113.301826](https://doi.org/10.1161/ATVBAHA.113.301826).
- ⁸¹Yamamoto, K., C. D. Protack, G. Kuwahara, M. Tsuneki, T. Hashimoto, M. R. Hall, *et al.* Disturbed shear stress reduces Klf2 expression in arterial-venous fistulae in vivo. *Physiol. Rep.* 2015. doi:[10.14814/phy2.12348](https://doi.org/10.14814/phy2.12348).